Mechatronics 19 (2009) 1211–1220

Contents lists available at ScienceDirect

Mechatronics

journal homepage: www.elsevier.com/locate/mechatronics

The investigation of the maneuverability deterioration based on acceleration radius theory

Kuei-Jen Cheng, Pi-Ying Cheng *

Department of Mechanical Engineering, National Chiao-Tung University, 1001 University Road, Hsinchu City, Taiwan 300, ROC

ARTICLE INFO

Article history:
Received 23 September 2007
Accepted 27 March 2009

Keywords:
Maneuverability
Acceleration radius
Deterioration rate

ABSTRACT

Maneuverability is the measure of the dynamic performance of a manipulator in a specific posture or configuration, and acceleration radius is one of the most utilized indices of it. Acceleration radius can be utilized as the reference to judge whether further dynamic analysis should be performed when evaluating the controllability and feasibility of the manipulator following the prescribed path with assigned kinematic and kinetic requirements in the planning phase. When utilizing acceleration radius as the dynamic reference in the planning phase, it can prevent wasting the calculation cost due to these non-necessary dynamic analyses, and it can also be utilized as the benchmark in the on-line control.

However, the existence of the configuration errors is inevitable in reality, and it deteriorates the dynamic performance of a manipulator with the ideal configuration parameters and leads to the potential risk of failing to achieve an assigned dynamic task. To investigate the adverse behavior caused by the configuration errors and to provide some clues to avoid or reduce their influence, this article proposes a novel and systematic method which can be used to evaluate the maneuverability deterioration of a non-redundant serial manipulator system due to the influence of configuration errors, and it also provides an index, deterioration rate, to quantitate this kind of deterioration. Deterioration rate can be utilized to quantitate the maneuverability deterioration due to the influence of configuration errors in a prescribed workspace or region and can also be treated as the safety or derating margin when proceeding with the control or path planning.

1. Introduction

Acceleration radius is utilized to describe the ability of a manipulator to accelerate its end-effecter and defined as the maximum achievable acceleration in all directions of the end-effecter in a specific posture or configuration by the known output limits of joint actuators. For easily being understood, the definition of acceleration radius is briefly demonstrated in Fig. 1 with a two degrees of freedom example. Acceleration radius is one of the common indices of maneuverability which usually is utilized as the reference to judge whether further dynamic analysis should be performed in the planning phase to reduce the calculation cost and relieve the burden of a control or path designer when planning the control strategies or trajectories.

However, when manufacturing and assembling a manipulator, the existence of the configuration errors due to these processes is inevitable. Since acceleration radius is defined as the maximum achievable acceleration in all directions, it shall include the adverse influence due to the configuration errors in its mathematical model to prevent planning an unattainable or infeasible dynamic task.

In the 80s and the early 90s, the literature studied in this field discusses the best expression to present the maneuverability or how to calculate it with the fastest speed or the maximum efficiency [1–3]. In the 90s, the direction of the studies changed to investigate the maneuverability in the redundant robot systems and its application [4–9]. In the recent years, the study focused on what the influence of velocity has on the maneuverability [10–13]. Although lots of literature has been published in this field, none of them mentions the influence of configuration errors in their studies. This leads the conclusions to not fully match the reality. To redeem this insufficiency, this article conducts the mathematical model of the acceleration radius, which includes the influence of configuration errors, and proposes a systematic method to evaluate the maneuverability deterioration of a non-redundant serial manipulator due to the influence of these errors. Besides, this article also provides a new index, deterioration rate, to quantitatively express the maneuverability deterioration due to the influence of these configuration errors.

For effectively expressing the proposed method and index, this article is arranged as follows. The kinematics of a manipulator based on Denavit–Hartenberg transformation matrix (D–H transformation matrix) with configuration errors is conducted in Section 2. In Section 3, it interprets how to derive the acceleration

* Corresponding author. Tel.: +886 3 5712121 55131; fax: +886 3 5720634.
E-mail address: pycheng@cc.nctu.edu.tw (P.-Y. Cheng).

0957-4158/$ - see front matter © 2009 Elsevier Ltd. All rights reserved.
doi:10.1016/j.mechatronics.2009.03.011

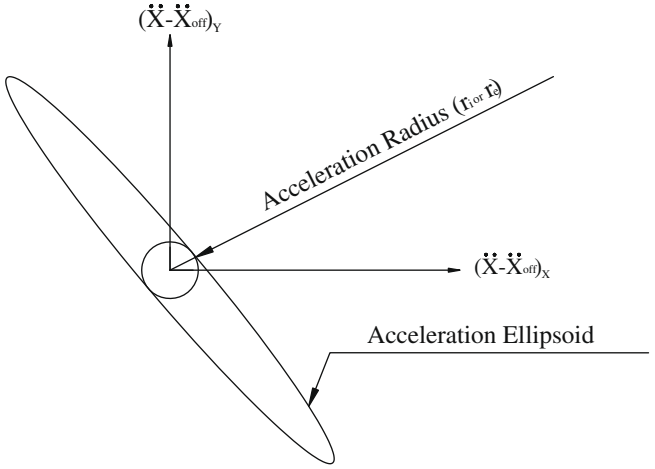

Fig. 1. Definition of the acceleration radius with a two degrees of freedom example.

ellipsoid and acceleration radius with the influence of configuration errors. In this section, the meaning and expression of deterioration rate is also interpreted. In Section 4, two examples are utilized to demonstrate the maneuverability deterioration due to the influence of configuration errors in the prescribed workspace. Some conclusions are presented in Section 5.

2. Kinematics with configuration errors

2.1. D–H Transformation matrix with configuration errors between two consecutive links

D–H transformation matrix is wildly used in kinematic analysis of the serial type manipulator. Between two consecutive links, link $i-1$ and i, D–H transformation matrix can be determined by four D–H link parameters, θ_i, d_i, a_i, and α_i, as shown in Fig. 2 [14].

From the definitions of D–H link parameters demonstrated in Fig. 2 and [14], the standard form of D–H matrix, ${}^{i-1}A_i^{SDH}$, can be expressed as (1).

$$ {}^{i-1}A_i^{SDH} = \begin{bmatrix} C\theta_i & -S\theta_i C\alpha_i & S\theta_i S\alpha_i & a_i C\theta_i \\ S\theta_i & C\theta_i C\alpha_i & -C\theta_i S\alpha_i & a_i S\theta_i \\ 0 & S\alpha_i & C\alpha_i & d_i \\ 0 & 0 & 0 & 1 \end{bmatrix} \tag{1} $$

However, when configuration errors exist in the manipulator, the standard D–H transformation matrix can not fully describe the whole system due to the angle error of the rotation about the y_i axis which can not be compensated or covered with reasonable values by other standard D–H link parameters when the orientations of the two consecutive joint axes are parallel or near parallel [15–18]. For this reason, another link parameter, β_i, which is the rotation angle about the y_i axis as shown in Fig. 2 must be introduced into the standard D–H transformation matrix to redeem this insufficiency. It must be emphasized that the necessity of β_i is only held when the orientations of two consecutive joint axes are parallel or near parallel. Except the condition stated above, the standard D–H transformation matrix can fully describe the whole system with configuration errors. The reason for putting β_i into the discussion is to get the general form of a manipulator system with configuration errors. In any case, β_i is always set to be zero, and only its error, $\Delta\beta_i$ will be used and discussed.

The modified D–H transformation matrix, ${}^{i-1}A_i$, aims to redeem the insufficiency stated above and is conducted by post-multiplying the standard D–H transformation matrix, ${}^{i-1}A_i^{SDH}$, with the rotation homogeneous matrix of β_i as shown in (2).

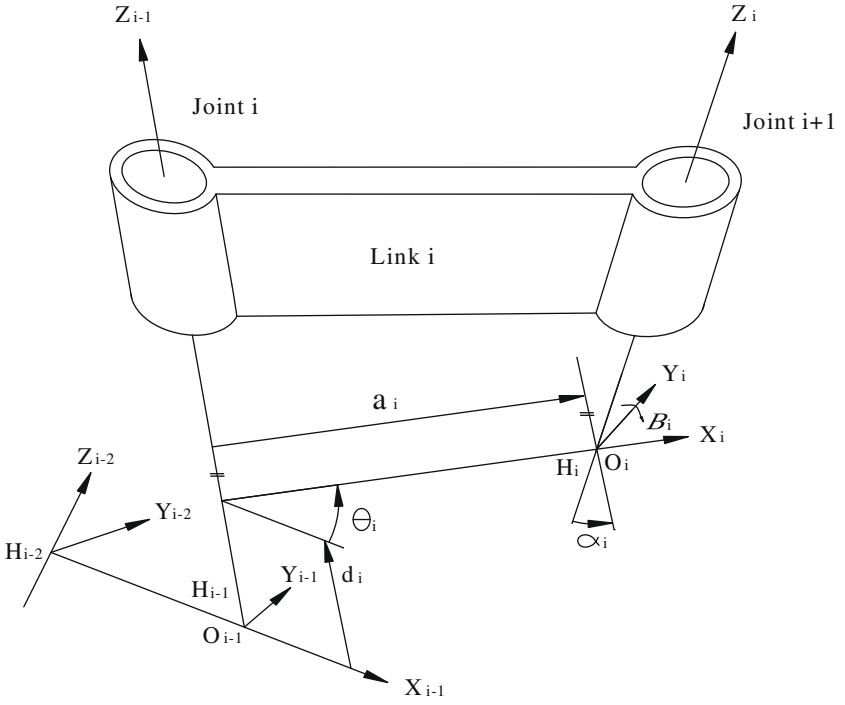

Fig. 2. Definitions of D–H link parameters.

$$
\begin{aligned}
{}^{i-1}A_i &= {}^{i-1}A_i^{SDH}A(y_i,\beta_i)\\
&= \begin{bmatrix} C\theta_i & -S\theta_iC\alpha_i & S\theta_iS\alpha_i & a_iC\theta_i\\ S\theta_i & C\theta_iC\alpha_i & -C\theta_iS\alpha_i & a_iS\theta_i\\ 0 & S\alpha_i & C\alpha_i & d_i\\ 0 & 0 & 0 & 1 \end{bmatrix}\begin{bmatrix} C\beta_i & 0 & -S\beta_i & 0\\ 0 & 1 & 0 & 0\\ S\beta_i & 0 & C\beta_i & 0\\ 0 & 0 & 0 & 1 \end{bmatrix}\\
&= \begin{bmatrix} C\theta_iC\beta_i - S\theta_iS\alpha_iS\beta_i & -S\theta_iC\alpha_i & C\theta_iS\beta_i + S\theta_iS\alpha_iC\beta_i & a_iC\theta_i\\ S\theta_iC\beta_i + C\theta_iS\alpha_iS\beta_i & C\theta_iC\alpha_i & S\theta_iS\beta_i - C\theta_iS\alpha_iC\beta_i & a_iS\theta_i\\ -C\alpha_iS\beta_i & S\alpha_i & C\alpha_iC\beta_i & d_i\\ 0 & 0 & 0 & 1 \end{bmatrix}
\end{aligned}
\tag{2}
$$

where $A(y_i, \beta_i)$ is the rotation homogeneous matrix of β_i. When β_i is equal to zero, (2) is fully equivalent to the standard D–H transformation matrix. When configuration errors exist, the corrective modified D–H transformation matrix that includes configuration errors can be expressed as the sum of the original modified D–H transformation matrix and the differential change matrix which is due to the influence of these errors [16] and shown in (3).

$$
{}^{i-1}A_i^C = {}^{i-1}A_i + dA_i \tag{3}
$$

where ${}^{i-1}A_i^C$ is the corrective modified D–H transformation matrix, ${}^{i-1}A_i$ is the modified D–H transformation matrix with nominal D–H link parameters, and dA_i is the differential change matrix due to the influence of configuration errors. Because β_i is always set to be zero, then $C\beta_i = 1$ and $S\beta_i = 0$. Setting $\Delta\theta_i$, Δd_i, Δa_i, $\Delta\alpha_i$, and $\Delta\beta_i$ are the errors of θ_i, d_i, a_i, α_i, and β_i, respectively. Because these errors are always much smaller than the nominal design link parameters, dA_i can be presented as the linear combination of these errors, as shown in (4).

$$
dA_i = \frac{\partial A_i}{\partial\theta_i}\Delta\theta_i + \frac{\partial A_i}{\partial d_i}\Delta d_i + \frac{\partial A_i}{\partial a_i}\Delta a_i + \frac{\partial A_i}{\partial\alpha_i}\Delta\alpha_i + \frac{\partial A_i}{\partial\beta_i}\Delta\beta_i \tag{4}
$$

Set $\frac{\partial A_i}{\partial\theta_i} = D_\theta{}^{i-1}A_i, \frac{\partial A_i}{\partial d_i} = D_d{}^{i-1}A_i, \frac{\partial A_i}{\partial a_i} = D_a{}^{i-1}A_i, \frac{\partial A_i}{\partial\alpha_i} = D_\alpha{}^{i-1}A_i$, and $\frac{\partial A_i}{\partial\beta_i} = D_\beta{}^{i-1}A_i$,where

$$
D_\theta = \begin{bmatrix} 0 & -1 & 0 & 0\\ 1 & 0 & 0 & 0\\ 0 & 0 & 0 & 0\\ 0 & 0 & 0 & 0 \end{bmatrix},\quad D_d = \begin{bmatrix} 0 & 0 & 0 & 0\\ 0 & 0 & 0 & 0\\ 0 & 0 & 0 & 1\\ 0 & 0 & 0 & 0 \end{bmatrix},
$$

$$
D_a = \begin{bmatrix} 0 & 0 & S\theta_i & -d_iS\theta_i\\ 0 & 0 & -C\theta_i & d_iC\theta_i\\ -S\theta_i & C\theta_i & 0 & 0\\ 0 & 0 & 0 & 0 \end{bmatrix},\quad D_\alpha = \begin{bmatrix} 0 & 0 & 0 & C\theta_i\\ 0 & 0 & 0 & S\theta_i\\ 0 & 0 & 0 & 0\\ 0 & 0 & 0 & 0 \end{bmatrix},
$$

$$
D_\beta = \begin{bmatrix} 0 & -S\alpha_i & C\theta_iC\alpha_i & a_iS\theta_iS\alpha_i - d_iC\theta_iC\alpha_i\\ S\alpha_i & 0 & S\theta_iC\alpha_i & -a_iC\theta_iS\alpha_i - d_iS\theta_iC\alpha_i\\ -C\theta_iC\alpha_i & -S\theta_iC\alpha_i & 0 & a_iC\alpha_i\\ 0 & 0 & 0 & 0 \end{bmatrix}
$$

From (4),

$$
dA_i = \left(D_\theta\Delta\theta_i + D_d\Delta d_i + D_a\Delta a_i + D_\alpha\Delta\alpha_i + D_\beta\Delta\beta_i\right){}^{i-1}A_i \tag{5}
$$

Set $\delta^{i-1}A_i = D_\theta\Delta\theta_i + D_d\Delta d_i + D_a\Delta a_i + D_\alpha\Delta\alpha_i + D_\beta\Delta\beta_i$, then the corrective modified D–H transformation matrix can be expressed as (6).

$$
{}^{i-1}A_i^C = {}^{i-1}A_i + d^{i-1}A_i = {}^{i-1}A_i + (\delta^{i-1}A_i)^{i-1}A_i \tag{6}
$$

where

$$
\begin{aligned}
\delta^{i-1}A_i = &\begin{bmatrix} 0 & -\Delta\theta_i & S\theta_i\Delta a_i & C\theta_i\Delta\alpha_i - d_iS\theta_i\Delta a_i\\ \Delta\theta_i & 0 & -C\theta_i\Delta a_i & S\theta_i\Delta\alpha_i + d_iC\theta_i\Delta a_i\\ -S\theta_i\Delta a_i & C\theta_i\Delta a_i & 0 & \Delta d_i\\ 0 & 0 & 0 & 0 \end{bmatrix}\\
&+\begin{bmatrix} 0 & -S\alpha_i\Delta\beta_i & C\theta_iC\alpha_i\Delta\beta_i & (a_iS\theta_iS\alpha_i - d_iC\theta_iC\alpha_i)\Delta\beta_i\\ S\alpha_i\Delta\beta_i & 0 & S\theta_iC\alpha_i\Delta\beta_i & (-a_iC\theta_iS\alpha_i - d_iS\theta_iC\alpha_i)\Delta\beta_i\\ -C\theta_iC\alpha_i\Delta\beta_i & -S\theta_iC\alpha_i\Delta\beta_i & 0 & a_iC\alpha_i\Delta\beta_i\\ 0 & 0 & 0 & 0 \end{bmatrix}
\end{aligned}
$$

2.2. Total transformation matrix with configuration errors

From (6), the corrective modified D–H transformation matrix of two consecutive links can also be presented as (7).

$$
{}^{i-1}A_i^C = (I + \delta^{i-1}A_i)^{i-1}A_i \tag{7}
$$

where I is the 4×4 identical matrix. From (7), the total corrective modified D–H transformation matrix, T_n^C, can be presented as (8).

$$
T_n^C = \prod_{i=1}^{n}{}^{i-1}A_i^C = \prod_{i=1}^{n}(I + \delta^{i-1}A_i)^{i-1}A_i \tag{8}
$$

where n is the number of the consisting links.

Because the kinematic deviation due to the error items, $\delta^{i-1}A_i$, is relatively small, the influence of the second and higher order terms can be omitted without any significant influence on the result. In the following, only the first order approximation of (8) will be utilized, and it can be presented as (9).

$$
\begin{aligned}
T_n^C &= T_n + \sum_{i=1}^{n}T_{i-1}\delta^{i-1}A_i{}^iT_n = \left(I + \sum_{i=1}^{n}T_{i-1}\delta^{i-1}A_iT_{i-1}^{-1}\right)T_n\\
&= \begin{bmatrix} R_n^C & P_n^C\\ 0 & 1 \end{bmatrix} = \begin{bmatrix} R_n + \left(\sum_{i=1}^{n}R_{i-1}\delta r_iR_{i-1}^{-1}\right)R_n & P_n + \left[\sum_{i=1}^{n}(R_{i-1}\delta r_iR_{i-1}^{-1})\right]P_n - \sum_{i=1}^{n}\left(R_{i-1}\delta r_iR_{i-1}^{-1}P_{i-1} - R_{i-1}\delta p_i\right)\\ 0 & 1 \end{bmatrix}\\
&= \begin{bmatrix} \left[I + \left(\sum_{i=1}^{n}R_{i-1}\delta r_iR_{i-1}^{-1}\right)\right]R_n & \left[I + \sum_{i=1}^{n}\left(R_{i-1}\delta r_iR_{i-1}^{-1}\right)\right]P_n - \sum_{i=1}^{n}\left(R_{i-1}\delta r_iR_{i-1}^{-1}P_{i-1} - R_{i-1}\delta p_i\right)\\ 0 & 1 \end{bmatrix}
\end{aligned}
\tag{9}
$$

2.3. Jacobian matrix with configuration errors

Jacobian matrix is utilized to map the joint velocities in the joint space into the end-effecter velocity in the world space. In the general form, it can be shown as (10).

$$
\dot{x}_n = \begin{bmatrix} v_n\\ w_n \end{bmatrix} = J_{n\times n}\dot{q}_n \tag{10}
$$

where n is the dimension of joint and end-effecter velocities in their corresponding spaces, v_n is the linear velocity vector and w_n is the angular velocity vector of end-effecter in the world space, $J_{n\times n}$ is the $n \times n$ Jacobian matrix, and $\dot{q}_n$ is the joint velocity vector in the joint space. In (11) and (12), they show v_n and w_n, respectively [19].

$$
v_n = \sum_{i=1}^{n}\left[\dot{\theta}_i(z_{i-1}^C \times {}^{i-1}p_n^C) + z_{i-1}^C\dot{d}_i\right] \tag{11}
$$

$$w_n = \sum_{i=1}^{n} \dot{\theta}_i z_{i-1}^C \tag{12}$$

where z_{i-1}^C is the z axis direction of the $i-1$ frame which is described in the reference frame and equivalent to the 3rd column vector of R_{i-1}^C, ${}^{i-1}p_n^C$ is the corrective position vector from end-effecter to the origin of the $i-1$ frame and is also described in the reference frame, $\dot{\theta}_i$ is the angular velocity value of the ith revolute joint, and $\dot{d}_i$ is the linear velocity value of the ith prismatic joint.

From the conduction in (9), z_{i-1}^C and ${}^{i-1}p_n^C$ can be presented as (13) and (14), respectively.

$$z_{i-1}^C = z_{i-1} + \left[\left(\sum_{j=1}^{i-1} R_{j-1}\delta r_j R_{j-1}^{-1}\right) R_{i-1}\right]_z \tag{13}$$

$$\begin{aligned}
{}^{i-1}P_n^C &= R_{i-1}[{}^{i-1}T_n]_P + R_{i-1}[d^{i-1}T_n]_P + dR_{i-1}[{}^{i-1}T_n]_P + dR_{i-1}[d^{i-1}T_n]_P \\
&= {}^{i-1}P_n + R_{i-1}\left[\left(\sum_{j=i}^{n} {}^{i-1}T_{j-1}\delta^{j-1}A_j{}^{i-1}T_{j-1}^{-1}\right){}^{i-1}T_n\right]_P \\
&\quad + \left[\left(\sum_{j=1}^{i-1} R_{j-1}\delta r_j R_{j-1}^{-1}\right) R_{i-1}\right][{}^{i-1}T_n]_P \\
&\quad + \left[\left(\sum_{j=1}^{i-1} R_{j-1}\delta r_j R_{j-1}^{-1}\right) R_{i-1}\right]\left[\left(\sum_{j=i}^{n} {}^{i-1}T_{j-1}\delta^{j-1}A_j{}^{i-1}T_{j-1}^{-1}\right){}^{i-1}T_n\right]_P
\end{aligned} \tag{14}$$

where z_{i-1} is the z axis direction of the $i-1$ frame presented in the reference frame which is equivalent to the 3rd column vector of R_{i-1}, ${}^{i-1}p_n$ is the position vector from end-effecter to the origin of the $i-1$ frame and also is described in the reference frame, and δr_j is the rotational part of $\delta^{j-1}A_j$. The subscript "P" means the translation part of the bracketed transformation matrix and the subscript "Z" means the z axis direction of the bracketed rotation matrix equivalent to the 3rd column vector.

From (10)–(12), the corrective Jacobian matrix can be expressed as (15).

$$J^C = \left[J_1^C, J_2^C, \ldots, J_n^C\right] \tag{15}$$

where $J_i^C = \begin{bmatrix} z_{i-1}^C \times {}^{i-1}p_n^C \\ z_{i-1}^C \end{bmatrix}$ is for a revolution joint, and $J_i^C = \begin{bmatrix} z_{i-1}^C \\ 0 \end{bmatrix}$ is for a prismatic joint.

Substitute (13) and (14) into (15) and eliminate the second order term, J_i^C can be presented as (16).

$$J_i^C = J_i + dJ_i \tag{16}$$

where J_i is the ith column of the nominal Jacobian matrix without the influence of configuration errors, and dJ_i is the differential change Jacobian matrix due to the influence of these errors.

In (17) and (18), they show J_i and the first order dJ_i of a revolute joint, respectively.

$$J_i = \begin{bmatrix} z_{i-1} \times {}^{i-1}p_n \\ z_{i-1} \end{bmatrix} \tag{17}$$

$$dJ_i = \begin{bmatrix} z_{i-1} \times P_e + z_{de} \times {}^{i-1}P_n \\ z_{de} \end{bmatrix} \tag{18}$$

Similarly, in (19) and (20), they represent J_i and dJ_i of a prismatic joint, respectively.

$$J_i = \begin{bmatrix} z_{i-1} \\ 0 \end{bmatrix} \tag{19}$$

$$dJ_i = \begin{bmatrix} z_{de} \\ 0 \end{bmatrix} \tag{20}$$

where $z_{de} = \left[\left(\sum_{j=1}^{i-1} R_{j-1}\delta r_j R_{j-1}^{-1}\right) R_{i-1}\right]_z$ is the direction error of the z axis of the $i-1$ frame, and $P_e = R_{i-1}\left[\left(\sum_{j=i}^{n} {}^{i-1}T_{j-1}\delta^{j-1}A_j{}^{i-1}T_{j-1}^{-1}\right){}^{i-1}T_n\right]_P + \left[\left(\sum_{j=1}^{i-1} R_{j-1}\delta r_j R_{j-1}^{-1}\right) R_{i-1}\right][{}^{i-1}T_n]_P + \left[\left(\sum_{j=1}^{i-1} R_{j-1}\delta r_j R_{j-1}^{-1}\right) R_{i-1}\right]\left[\left(\sum_{j=i}^{n} {}^{i-1}T_{j-1}\right.\right.$ $\left.\left.\delta^{j-1}A_j{}^{i-1}T_{j-1}^{-1}\right){}^{i-1}T_n\right]_P$ is the position error due to the influence of configuration errors from the end-effecter to the $i-1$ link.

3. Acceleration radius with configuration errors

The first and second order differential kinematic equations of the end-effecter of a non-redundant serial manipulator can be expressed as (21) and (22) [2,3].

$$\dot{x}_n = J_{n\times n}^C(q)\dot{q}_n \tag{21}$$

$$\ddot{x}_n = \dot{J}_{n\times n}^C(q)\dot{q}_n + J_{n\times n}^C(q)\ddot{q}_n \tag{22}$$

where q is the joint variable, x is the position variable of the end-effecter, and $J_{n\times n}^C$ is the $n\times n$ corrective Jacobian matrix.

The dynamic equation of a manipulator can be presented as (23).

$$\tau = M(q)\ddot{q} + c(q,\dot{q}) + g(q) \tag{23}$$

where $\tau \in R^n$ is the vector of the joint forces, torques, or both, $M(q) \in R^{n\times n}$ is the symmetric, positive definite inertia matrix, $c(q,\dot{q}) \in R^n$ is the vector of the centrifugal and Coriolis forces, torques, or both, and $g(q) \in R^n$ is the vector of the external forces, torques, or both.Rearrange (23), the $\ddot{q}$ can be presented as (24).

$$\ddot{q} = M^{-1}(\tau - c - g) \tag{24}$$

Substitute (24) into (22), $\ddot{x}$ can be presented as (25).

$$\begin{aligned}
\ddot{x} &= J^C M^{-1}(\tau - c - g) + \dot{J}^C\dot{q} \\
&= J^C M^{-1}\tau + (-J^C M^{-1}c + \dot{J}^C\dot{q}) + (-J^C M^{-1}g) = J^C M^{-1}\tau + \ddot{x}_{off}
\end{aligned} \tag{25}$$

where $\ddot{x}$ is the acceleration vector of the end-effecter, $J^C M^{-1}\tau$ is the acceleration vector which is contributed by the actuation of each consisting joint actuator, and $\ddot{x}_{off} = (-J^C M^{-1}c + \dot{J}^C\dot{q}) + (-J^C M^{-1}g)$ is the acceleration vector due to the linear velocity, angular velocity, external force and torque exists in each consisting link.

Usually, the output torque or force of each joint actuator has symmetric upper and lower limits and can be expressed as (26).

$$-\tau_i^{\lim\ it} \leqslant \tau_i \leqslant \tau_i^{\lim\ it}, \quad i = 1 \sim n \tag{26}$$

After normalizing, the normalized output vector, $\hat{\tau}$, can be presented as (27).

$$\hat{\tau} = L^{-1}\tau \tag{27}$$

where L is the diagonal matrix which the value of each diagonal element is equal to the output limit of the corresponding joint actuator and is expressed as (28).

$$L = \begin{bmatrix} \tau_i^{\lim\ it} & 0 & 0 \\ 0 & \ddots & 0 \\ 0 & 0 & \tau_n^{\lim\ it} \end{bmatrix} \tag{28}$$

From (26) and (27), $\hat{\tau}$ has the characteristics as shown in (29) and (30).

$$|\hat{\tau}| \leqslant 1 \tag{29}$$

$$\hat{\tau}^T\hat{\tau} \leqslant 1 \tag{30}$$

Substitute (27) into (25) and then rearrange, $\ddot{x}$ and $\ddot{\tau}$ can be presented as (31) and (32), respectively.

$$\ddot{x} = JM^{-1}L\hat{\tau} + \ddot{x}_{off} \tag{31}$$

$$\hat{\tau} = L^{-1}MJ^{-1}(\ddot{x} - \ddot{x}_{off}) \tag{32}$$

Substitute (32) into (30), the equation of the acceleration ellipsoid can be conducted and expressed as (33).

$$(\ddot{x}-\ddot{x}_{off})^T J^{-T} M^T L^{-T} L^{-1} M J^{-1} (\ddot{x}-\ddot{x}_{off}) \leqslant 1 \quad (33)$$

Substitute $Q = J^{-T} M^T L^{-T} L^{-1} M J^{-1}$ into (33), a simpler form can be presented in (34).

$$(\ddot{x}-\ddot{x}_{off})^T Q (\ddot{x}-\ddot{x}_{off}) \leqslant 1 \quad (34)$$

The value of acceleration radius is equal to the value of the radius of the smallest inner tangent sphere of the acceleration ellipsoid which is centered in the origin of the reference frame. When $\ddot{x}_{off} = 0$, the acceleration radius is equal to the reciprocal of the square root of the largest eigenvalue of Q. If the value of the acceleration radius is less than the prescribed acceleration at some point of the path in planning or operation, this manipulator may not perform its assigned dynamic task due to the insufficient acceleration ability at this posture or configuration. This means further dynamic analysis should be performed to judge the assigned dynamic task at this posture or configuration is not toward these directions without sufficient acceleration ability to assure the assigned dynamic requirements are achievable.

For reasonably and effectively quantitating the adverse maneuverability deviation due to the influence of configuration errors and being as the derating margin of the manipulation, a new index, deterioration rate, is proposed and defined in (35).

$$DR_P = \frac{r_i - r_e}{r_i} \quad (35)$$

where DR_P is the deterioration rate at a specific posture or configuration, r_i and r_e are the acceleration radius without and with configuration errors, respectively.

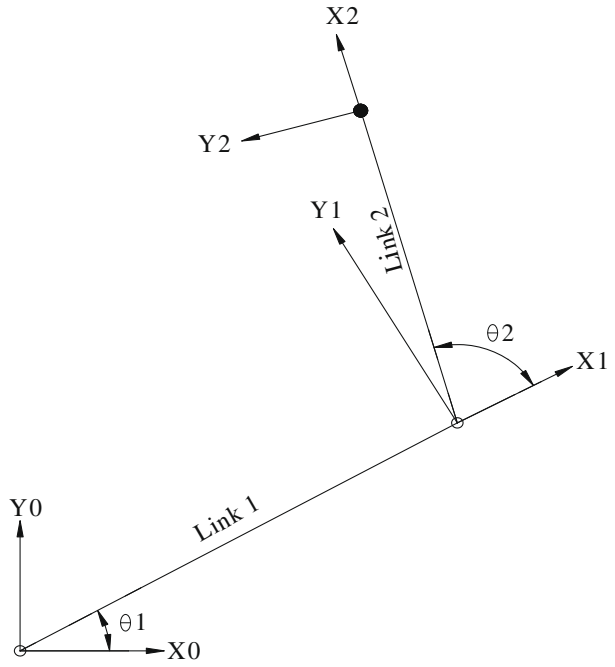

Fig. 3. Link parameter definitions of the two-link planar manipulator.

For a small workspace or region, a representative index of derating margin of manipulation over this workspace or region is useful, and this index can be expressed as (36) [3].

$$DR_W = \frac{I}{W} \quad (36)$$

where DR_W is the deterioration rate in a prescribed workspace or region, $I = \int_w (dr) dw$ is the integral of deterioration rate over this workspace or region, $W = \int_w dw$ presents the workspace or region in discussion, dr is the differential function of deterioration rate, and dw presents the differential of the workspace or region.When in application, the exact derating margin of manipulation at a specific posture or configuration must be represented by DR_P, but when roughly estimating the derating margin for a region, DR_W would be a better choice to reduce the cost and effort of judgment. When the prescribed workspace or region is a specific posture or configuration, DR_P and DR_W will be equivalent.

4. Examples

In this section, a two-link planar manipulator and a PUMA 560 robotic arm will be taken as the examples to demonstrate the proposed method and the maneuverability deterioration due to the prescribed configuration errors which usually can be found as the uncertainty or tolerance in the product specification. From (34), it is easy to find the influences caused by the centrifugal force, Coriolis force, gravity force, external force and torque just simply shift the center of the acceleration ellipsoid and can be easily reintroduced into the conducted results by the basic definition of acceleration radius. To simplify, both examples discussed in this section are assumed in standing, $\dot{q} = 0$ and omitted the influences of external forces and torques.

4.1. Two-link planar manipulator

The first example is to evaluate the maneuverability deterioration of a two-link planar manipulator which usually can be used to simulate the motion of arms or legs of a human being and shown in Fig. 3. Because the inverse Jacobian matrix does not exist when

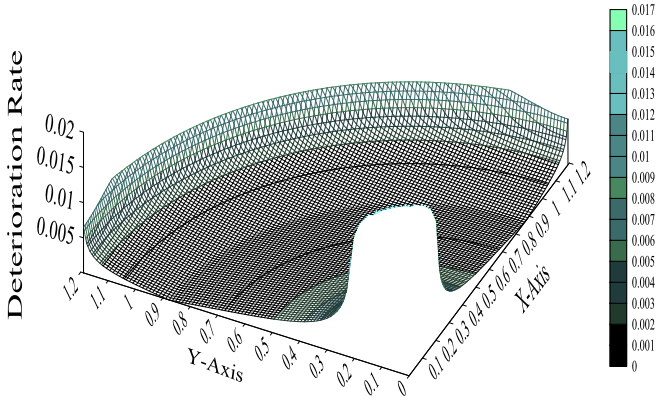

Fig. 4a. Deterioration rate distribution of Example 1 (a) 3D plot.

Table 1
Prescribed inertia properties, errors, and D–H parameters of the two links planar manipulator.

Link i	Link parameters							Errors				
	d	θ	a	α	β	Weight	Torque limits	Δd	$\Delta\theta$	Δa	$\Delta\alpha$	$\Delta\beta$
1	0	θ_1	0.7	0	0	3.5	±5	0	±0.1°	±0.0007	0	0

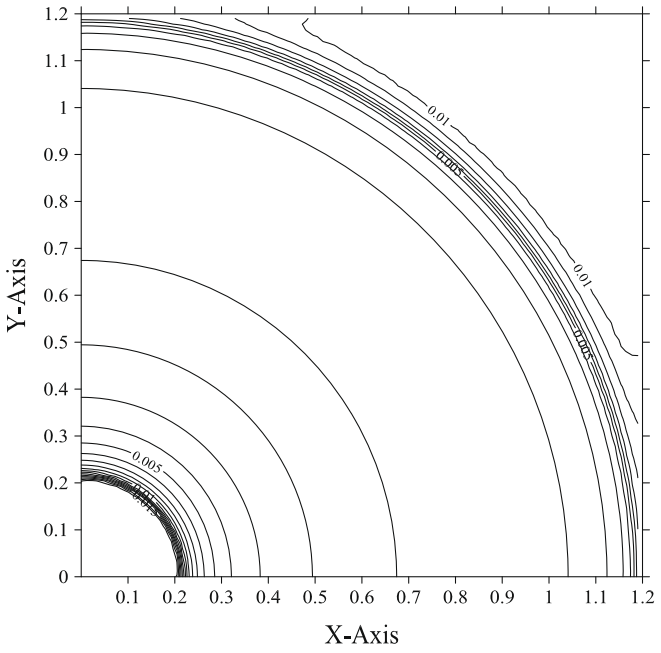

Fig. 4b. Deterioration rate distribution of Example 1 (b) Contour plot.

near or in the singular posture or configuration, in this example, it evaluates the maneuverability deterioration over a region which is slightly smaller than the real achievable workspace in the first quadrant. In Table 1, the setting of the inertia properties, configuration errors, and link parameters are presented. After taking all the settings presented in Table 1 into the proposed method, the deterioration rate of this region is derived, and its value is 0.16% which can be used as the rough estimation of derating margin of this region. The distribution of the deterioration rate is demonstrated in Figs. 4a and b and this distribution can be used as the exact reference of the derating margin of any posture or configuration in this region. In Figs. 4a and b, two phenomena can be observed easily. One is when the manipulator gets closer to the singular posture or configuration (the boundaries), no matter full stretched or folded, the deterioration rate becomes greater with the same configuration errors. The other is with the same distance between the end-effecter and base joint, the deterioration rate will also be the same, and this phenomenon implicitly means the value of θ_1 has no influence on the deterioration rate.

To further investigate these observations, the analytical forms of the acceleration radius and its sensitivity with regard to θ_2 of this example are conducted and shown in (37) and (38), respectively.

$$\text{Acceleration radius} = \frac{P_1}{\sqrt{\frac{P_2}{P_3} + \sqrt{\frac{P_2}{P_3^2} - \frac{P_4}{0.1225 P_3}}}} \tag{37}$$

$$\begin{aligned}&\text{Sensitivity with regard to } \theta_2 \\ &= \partial_{\theta_2} \frac{P_1}{\sqrt{\frac{P_2}{P_3} + \sqrt{\frac{P_2}{P_3^2} - \frac{P_4}{0.1225 P_3}}}} \\ &= -\left(\frac{P_7}{P_5} - \frac{2 \cdot P_8 \cdot P_9 \cdot P_6}{P_5^3} + \frac{\left(-P_{14} \cdot \frac{1}{P_5} - P_{15} \frac{P_6^2}{P_5^3} + \frac{P_6}{P_5} \left(P_9 + P_{16} \cdot \frac{1}{P_5^2} \right) \right)}{2 \cdot \sqrt{-\frac{P_{12}}{P_5^2} + \frac{P_8^2 P_9}{P_5^4}}} \right) \\ &= \frac{}{\sqrt{2} \cdot \left(\frac{P_8 \cdot P_9}{P_5^2} + \sqrt{-\frac{P_{12}}{P_5^2} + \frac{P_8^2 \cdot P_9}{P_5^4}} \right)^{\frac{3}{2}}}\end{aligned} \tag{38}$$

where $P_1 = \sqrt{2}$, $P_2 = 0.35430 - 0.00286 \cos\theta_2$, $P_3 = 0.1225 \sin^2\theta_2$, $P_4 = 0.00085$, $P_5 = \sin\theta_2$, $P_6 = \cos\theta_2$, $P_7 = 0.02332$, $P_8 = 8.16327$, $P_9 = 0.35430 - 0.00286 \cos\theta_2$, $P_{10} = 0.11334$, $P_{11} = 0.19038$, and $P_{12} = 0.05667$.

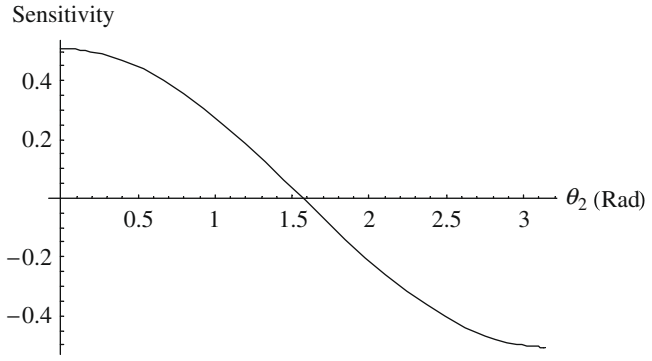

Fig. 5. Sensitivity of acceleration radius with regard to θ_2 .

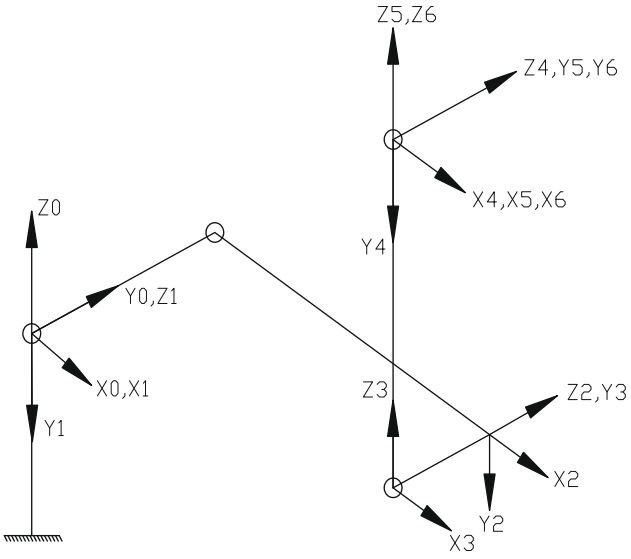

Fig. 6. Zero position with attached coordinate frames of PUMA 560.

From (37), it can easily be observed that no θ_1 item exists in the analytic form, and this means θ_1 has no influence on the acceleration radius. This matches the prior observation in this example. In Fig. 5, it shows the sensitivity of the acceleration radius with regard to θ_2, and the range of θ_2 is from 0 to π. From Fig. 5, it also can easily be observed that when θ_2 closes to 0 or π, it has the greatest sensitivity. This means when θ_2 closes to 0 or π, the same variation in θ_2 will cause greater deviation in the acceleration radius. In other words, when this manipulator is in full stretch or fold, configuration errors will have the greatest influence on maneuverability deterioration, and this matches the prior observation.

Table 2
D–H link parameters of PUMA 560.

Frame i	d_i (m)	θ_i (°)	a_i (m)	α_i (°)
1	0	θ_1	0	−90
2	0.2435	θ_2	0.4318	0
3	−0.0934	θ_3	0	90
4	0.4331	θ_4	−0.0203	−90
5	0	θ_5	0	90
6	0	θ_6	0	0

Table 3
Inertial parameters of each link of PUMA 560.

Link i	M (kg)	r_x (m)	r_y (m)	r_z (m)	I_{xx} (kg m^2)	I_{yy} (kg m^2)	I_{zz} (kg m^2)	$I_{xy} = I_{yz} = I_{zx;}$ (kg m^2)	Torque limit (N m)
1	0	0	0	0	0	0	0.35	0	±97.6
2	17.4	0.068	0.006	0.2275	0.13	0.524	0.539	0	±186.4
3	4.8	0	−0.070	−0.0794	0.066	0.0125	0.086	0	±89.4
4	0.82	0	−0.0203	0.4141	1.8×10^{-3}	1.8×10^{-3}	1.3×10^{-3}	0	±24.2
5	0.34	0	0	0.032	0.3×10^{-3}	0.3×10^{-3}	0.4×10^{-3}	0	±20.1
6	0.09	0	0	−0.064	0.15×10^{-3}	0.15×10^{-3}	0.04×10^{-3}	0	±21.3

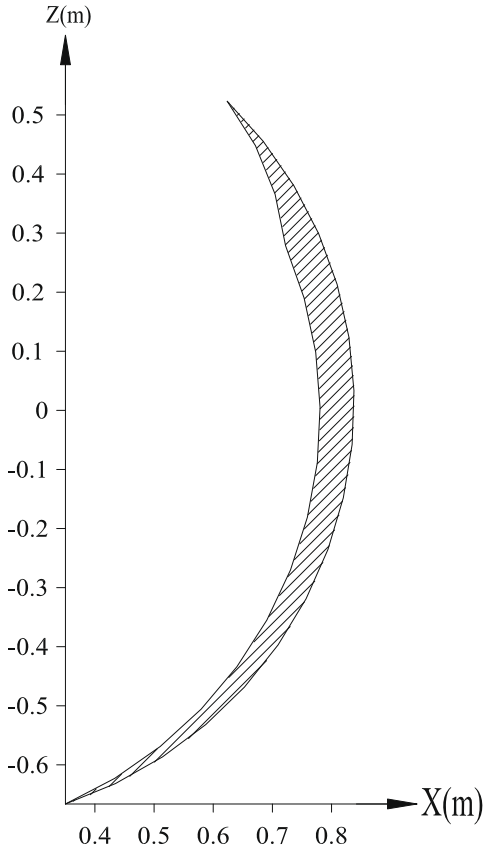

Fig. 7. Workspace of the designated joint regions of example 2.

4.2. PUMA 560

In the second example, it discusses the maneuverability deterioration due to the prescribed configuration errors of PUMA 560. The zero position with the attached frames of PUMA 560 is shown in Fig. 6, and its link parameters are shown in Table 2. In Table 3, the inertia and joint torque parameters of each link and its attached actuator are presented, respectively [20,21]. Because the design purpose of the wrist is dedicated to change the orientation of the end-effecter and not to be the kinetic functions provider, the configuration errors of the wrist will be omitted in the following discussion. Since θ_1 only changes the orientation of the acceleration ellipsoid without changing its shape, the value of θ_1 is independent of the acceleration radius [8]. Based on the reasons stated above, in the following discussion, only θ_2 and θ_3 will be taken as the control variables, and their ranges are specified in accordance with the one which covers most pick and place operations. Except θ_2 and θ_3, others will be taken as the constants, and their values will be explained as follows. For θ_4, θ_5, and θ_6, their values are 41°, 37°, and 16°, respectively for preventing the occurrence of the singular configurations in the discussed region. Also, in accordance with the capability of current precise machining technology, the values of the length and the angular errors are basically assigned as the 0.1% of the nominal dimensions and 0.1°, respectively.

Table 4
The prescribed configuration and its errors of case 1.

Link i	Parameters	Errors				
	θ	Δd	$\Delta\theta$	Δa	$\Delta\alpha$	$\Delta\beta$
1	0°	0	±0.1°	0	±0.1°	±0.1°
2	−45° to 45°	±0.00024	±0.1°	±0.00043	±0.1°	±0.1°
3	95°–135°	±0.00009	±0.1°	0	±0.1°	±0.1°
4	41°	±0.00043	0°	±0.00002	0°	0°
5	37°	0	0°	0	0°	0°
6	16°	0	0°	0	0°	0°

Table 5
The prescribed configuration and its errors of case 2.

Link i	Parameters	Errors				
	θ	Δd	$\Delta\theta$	Δa	$\Delta\alpha$	$\Delta\beta$
1	0°	0	±0.1°	0	±0.1°	0°
2	−45° to 45°	±0.00024	±0.1°	±0.00043	±0.1°	0°
3	95–135°	±0.00009	±0.1°	0	±0.1°	0°
4	41°	±0.00043	0°	±0.00002	0°	0°
5	37°	0	0°	0	0°	0°
6	16°	0	0°	0	0°	0°

Table 6
The prescribed configuration and its errors of case 3.

Link i	Parameters	Errors				
	θ	Δd	$\Delta\theta$	Δa	$\Delta\alpha$	$\Delta\beta$
1	0°	0	±0.5°	0	±0.5°	±0.5°
2	−45° to 45°	±0.00120	±0.5°	±0.00215	±0.5°	±0.5°
3	95–135°	±0.00045	±0.5°	0	±0.5°	±0.5°
4	41°	±0.00215	0°	±0.00010	0°	0°
5	37°	0	0°	0	0°	0°
6	16°	0	0°	0	0°	0°

For investigating the necessity of $\Delta\beta_i$, and the effect of the magnitude of the configuration errors to the deterioration rate, three cases are used to discuss these two issues in the following simulations. The link parameters and their errors of each case are presented in Tables 4–6, respectively, and the workspace under the discussed joint regions is shown in Fig. 7. From Figs. 8a and 9a, it can be observed that cases 1 and 2 have similar distributions of the deterioration rate, but case 2 has a much lower deterioration rate than the one in case 1. This phenomenon explicitly points out without including the effect of $\Delta\beta_i$ will lead to underestimate the deterioration rate, and this also shows the necessity of $\Delta\beta_i$

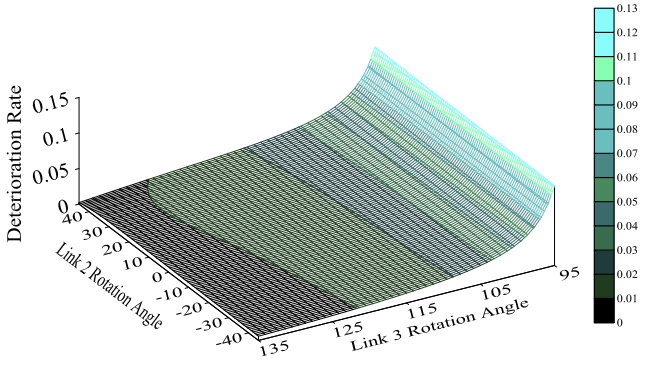

Fig. 8a. Deterioration rate distribution in the *X–Z* coordinates of case 1 (a) In the *X–Z* coordinates.

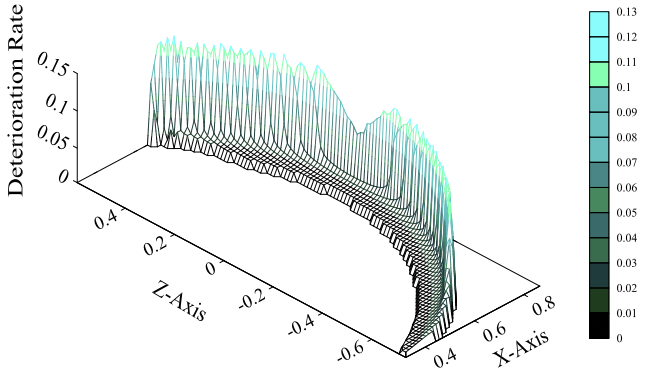

Fig. 8b. Deterioration rate distribution in the *X–Z* coordinates of case 1 (b) In θ_2 and θ_3 joints space.

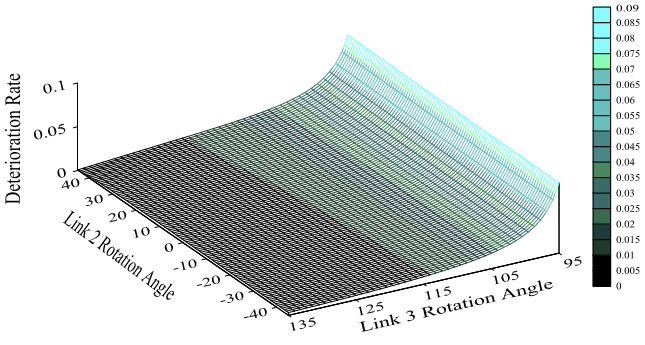

Fig. 9a. Deterioration rate distribution in the *X–Z* coordinates of case 2 (a) In the *X–Z* coordinates.

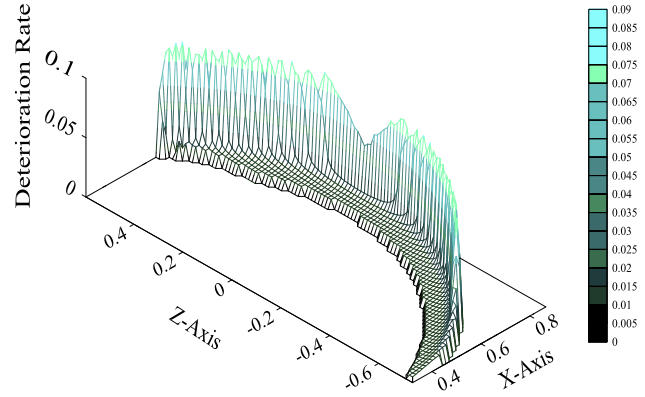

Fig. 9b. Deterioration rate distribution in the *X–Z* coordinates of case 2 (b) In θ_2 and θ_3 joints space.

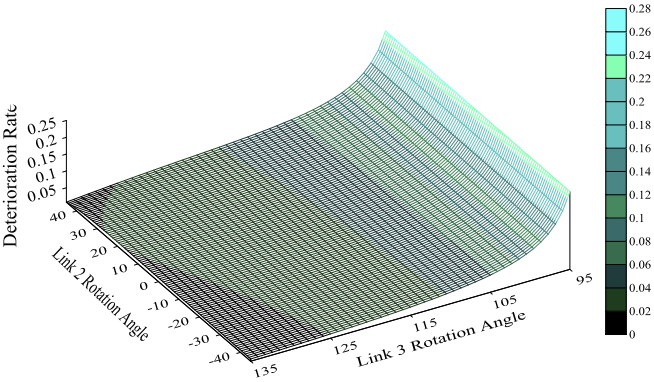

Fig. 10a. Deterioration rate distribution in the *X–Z* coordinates of case 3 (a) In the *X–Z* coordinates.

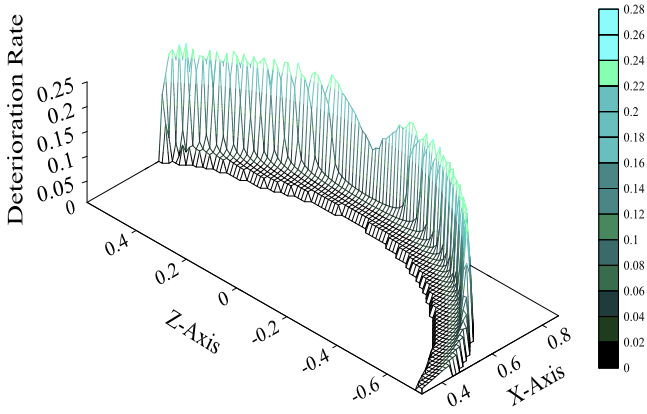

Fig. 10b. Deterioration rate distribution in the *X–Z* coordinates of case 3 (b) In θ_2 and θ_3 joints space.

when evaluating the configuration errors causing maneuverability deterioration of PUMA 560.

When observing Figs. 8a and 10a, these two diagrams also have similar distributions but different amplitudes. This phenomenon also means the magnitude of the configuration errors does influence the deterioration rate, and when the errors are greater, the greater deterioration rate will be.

From the above discussions, no matter the effect of $\Delta\beta_i$ is omitted, or the configuration errors are magnified, the distributions of the deterioration rates have similar trends but different amplitudes. This phenomenon can be deduced that the distribution of the maneuverability deterioration rate due to the influence of configuration errors mainly depends on the configuration of the discussed manipulator, but the actual amplitude is controlled by the magnitude of these errors and the configuration.

Besides, in Figs. 8a, 9a and 10a, one common phenomenon can be observed, and that is when θ_3 gets closer to 95° which is the outer boundary of the working region, the deterioration rate will be greater. In Fig. 11, it shows the two extreme configurations of

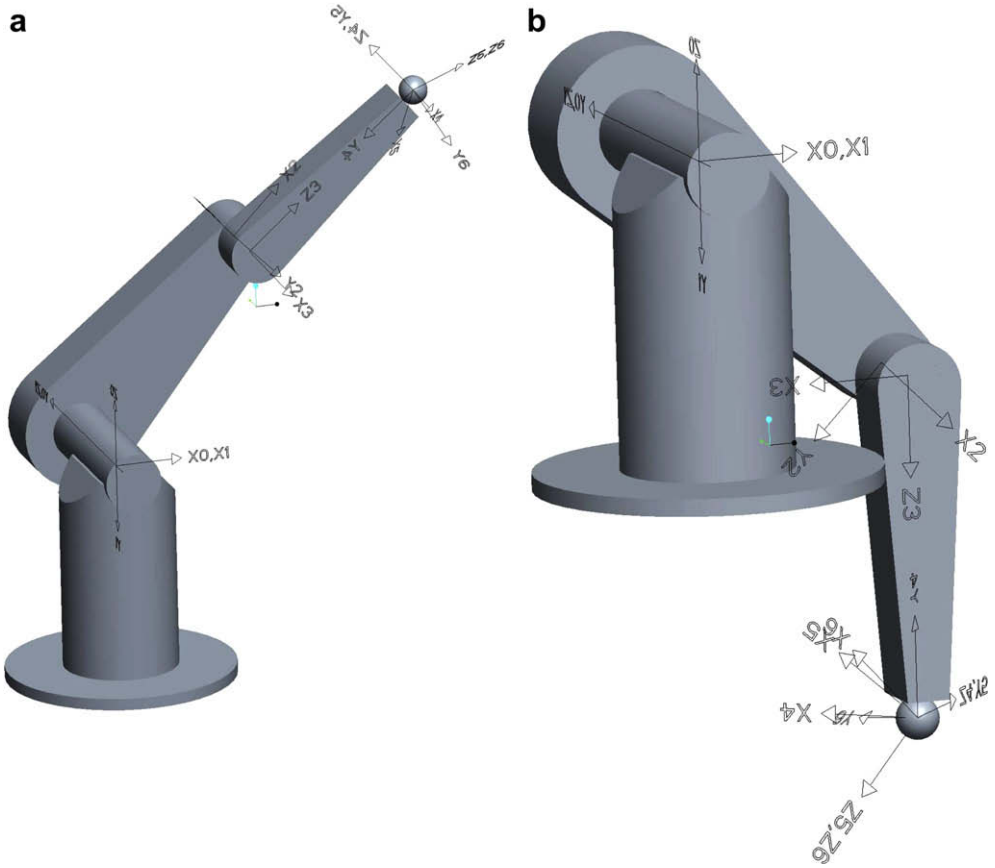

Fig. 11. Two extreme configurations of the discussed region (a) $\theta_2 = -45^\circ$ and $\theta_3 = 95^\circ$ (b) $\theta_2 = 45^\circ$ and $\theta_3 = 135^\circ$.

the discussed region which are located on the outer and inner boundaries. From Fig. 11a, it is easily observed that when $\theta_3 = 90^\circ$, this robotic arm is in a singular posture due to the full stretch between link 2 and link 3. Also from Fig. 11b, it can be found that when $\theta_3 = 135^\circ$, it is the posture or configuration that is far from the singular ones, no matter the one in full stretch or fold is and has smaller deterioration rate. From this observation, one deduction can be conducted, and that is even with the same configuration errors, when getting closer to the singular posture or configuration, the deterioration rate will be greater.

5. Conclusions

The existence of configuration errors is inevitable when manufacturing and assembling a manipulator. When evaluating the maneuverability of a manipulator system without including the influence of these errors, the system maneuverability will be overestimated and will cause system control failure or other unpredictable adverse outcomes especially in the high speed or relative heavy loading applications with kinetic or dynamic requirements, e.g. the limbs of a walking robot or a robot arm simulating a ball throw of a human arm. To redeem this insufficiency, this article proposes a systematic method to include the influence of configuration errors into the analytical model and proposes an index, deterioration rate, to quantitate the maneuverability deterioration due to the influence of these errors. By utilizing this index, it is easy for a control or path designer to assign a reasonable derating margin of manipulation to plan control strategies or trajectories to attain an assigned dynamic task without any potential failure risk caused by the maneuverability deterioration due to the influence of configuration errors.

From the observations found in Section 4, three conclusions can be conducted. The first one is when getting closer to the singular postures or configurations, the deterioration rate will be greater, even with the same configuration errors. The second is the distribution of the deterioration rate mainly depends on the configuration, but the actual amplitude is controlled by the magnitude of these errors and the configuration. The last one is that $\Delta\beta_i$ has its existence necessity when evaluating maneuverability deterioration due to the influence of configuration errors. When omitting the influence of $\Delta\beta_i$, it will lead to underestimate the deterioration and may cause some unpredictable adverse outcomes.

Based on these observations, for a control or path designer, it is better to choose the path or working region far from the singular postures or configurations when numerous ones are available to reduce the influence of configuration errors on maneuverability, and if choosing the one close to the singular postures or configurations is inevitable, greater derating margin must be kept when the control strategies or trajectories are implemented. From the observations in Section 4.1, when the implemented path or working region is short or small and far from the singular postures or configurations, DR_W is a good estimation of the derating margin for the entire path or region. However, when close to the singular postures or configurations is inevitable, DR_p must be investigated for all the segments or sections which are close to these singular postures or configurations to get the information of setting the derating margin to them.

In this article, it proposed a systematic method to evaluate the maneuverability deterioration due to the influence of configuration errors, and it also provides an index, deterioration rate, to quantitate the maneuverability deterioration due to the influence of these errors. The proposed method and index are useful for a

control or path designer to decide the derating margin of manipulation or choose the path or region with less influence of configuration errors to ensure the achievement of the assigned dynamic task in a prescribed workspace or region. The examples not only show the relations between the maneuverability deterioration and the configuration errors but also find the guideline to choose the best path or region when numerous ones are available, and all these make a great benefit to the control or path designers when they plan the control strategies or trajectories to achieve an assigned dynamic task.

References

[1] Tsuneo Yoshikawa. Manipulability of robotic mechanisms. Int J Robot Res 1985;4(2):3–9.

[2] Graettinger Timothy J. The acceleration radius-a global performance measure for robotic manipulators. IEEE J Robot Automat 1988;4(1):60–9.

[3] Gosselin C, Angeles J. A global performance index for the kinematic optimization of robotic manipulator. ASME J Mech Des 1991;113:220–6.

[4] Kim Kim-Kap, Yoon Yong-San. Trajectory planning of redundant robots by maximizing the moving acceleration radius. Robotica 1992;10:195–203.

[5] Choi Byoung Wook, Won Jon Hwa, Chung Myung Jin. Evaluation of dexterity measures for a 3-link planar redundant manipulator using constraint locus. IEEE Trans Robot Automat 1995;11(2):282–5.

[6] Doty Keith L, Claudio Melchiorri, Schwartz Eric M, Claudio Bonivento. Robot manipulability. IEEE Trans Robot Automat 1995;11(3):462–8.

[7] Pasquale Chiacchio. A new dynamic manipulability ellipsoid for redundant manipulators. Robotica 2000;18:381–97.

[8] Kovecses Jozsef, Fenton Robert G, Cleghorn William L. Effects of joint dynamics on the dynamic manipulability of geared robot manipulator, vol. 11. Pergamon Mechatronics; 2001. p. 43–58.

[9] Gravagne Ian A, Walker Ian D. Manipulability and force ellipsoids for continuum robot manipulators. In: Proceedings of the 2001 IEEE international conference on intelligent robots and systems; 2001. p. 304–11.

[10] Rosenstein Michael T, Grupen Roderic A. Velocity-dependent dynamic manipulability. In: Proceedings of the 2002 IEEE international conference on robotics and automation; 2002. p. 2424–9.

[11] Bowling Alan P, Khatib Oussama. The actuation efficiency – a measure of acceleration capability for non-redundant robotic manipulators. In: Proceedings of the 2003 IEEE international conference on intelligent robots and systems; 2003. p. 3325–30.

[12] Bowling Alan P, Oussama Khatib. The dynamic capability equations-a new tool for analyzing robotic manipulator performance. IEEE Trans Robot Automat 2005;21(1):115–23.

[13] Bowling Alan P, ChangHwan Kim. Velocity effects on robotic manipulator dynamic performance. ASME Trans Mech Des 2006;128:1236–45.

[14] Denavit J, Hartenberg RS. A kinematic notation for lower-pair mechanisms based on matrices. ASME J Appl Mech 1955;22:215–21.

[15] Hayati Samad A. Robot arm geometric link parameter estimation. In: Proceedings of the 22nd IEEE international conference on decision and control; 1983. p. 1477–83.

[16] Veitchegger WK, Wu Chi-Haur. Robot accuracy analysis based on kinematics. IEEE J Robot Automat 1986;2(3):171–9.

[17] Veitchegger WK, Wu Chi-Haur. Robot calibration and compensation. IEEE J Robot Automat 1988;4(6):643–56.

[18] Caenen JL, Angue JC. Identification of geometric and non geometric parameters of robots. In: Proceedings of the 1990 IEEE international conference on robotics and automation; 1990. p. 1032–7.

[19] Tsai Lung-Wen. Robot analysis, 1st ed., vol. 1. New York: John Wiley and Sons; 1999.

[20] Armstrong Brian, Khatib Qussama, Burdick Joe. The explicit dynamic model and inertial parameters of the PUMA 560 arm. In: Proceedings of the 1986 IEEE international conference on robotics and automation; 1986. p. 510–8.

[21] Mozaryn J, Kurek JE. Design of decoupled sliding mode control for the PUMA 560 robot manipulator, In: Proceedings of the third international workshop on robot motion and control RoMoCo 2002, Bukowy Dworek, Poland; 2002. p. 45–50.